ELSEVIER

Journal of Power Sources 85 (2000) 29–37

JOURNAL OF POWER SOURCES

www.elsevier.com/locate/jpowsour

Dissolution and precipitation reactions of lead sulfate in positive and negative electrodes in lead acid battery

Zen-ichiro Takehara

Department of Chemical Engineering, Faculty of Engineering, Kansai University, Suita, Osaka, 564-8680 Japan

Accepted 22 September 1999

Abstract

Several studies in the author's former laboratory at Kyoto University, have been reviewed on the dissolution–precipitation reactions on the electrodes in the lead acid battery. At the discharges of β-PbO_2 in the positive electrode and Pb in the negative electrode, $PbSO_4$ deposited on both electrode surfaces through the large supersaturation of Pb^{2+} ion. Thus, the discharge reactions of the positive and the negative electrodes proceeded smoothly, and the largest crystal size of $PbSO_4$ was obtained in 0.5–1.0 M H_2SO_4 with the largest Pb^{2+} ion concentration on the surface. The size of its $PbSO_4$ crystals became smaller at a higher current discharge through the formation of many of nuclei on the electrode surface. On the other hand, the charge reactions, which are the anodic oxidation of $PbSO_4$ at the positive electrode and the cathodic reduction of $PbSO_4$ at the negative electrode, did not proceed in the same way as the discharge reactions, because $PbSO_4$ is a large ionic crystal without electronic or ionic conductivities and its solubility is very low in sulfuric acid solutions. The reaction site is considered to be the interface between β-PbO_2 of the positive active material, or Pb of the negative active material, and $PbSO_4$. At such an interface, Pb^{2+} ions can be adequately supplied from the $PbSO_4$ crystal, and a charge-transfer reaction can occur on β-PbO_2 or Pb. The reaction rate depends on the electrochemical kinetics parameters, e.g., exchange charge-transfer rate, real area of the interface between PbO_2 or Pb and $PbSO_4$, and the mass-transfer in the narrow gap can be assumed to be like that of a thin layer cell. For the oxidation of $PbSO_4$ to ß-PbO_2, the charge-transfer process was the rate-determining step. For the reduction of $PbSO_4$ to Pb, the mass-transfer process was the rate-determining step. For both processes, it was concluded that a large crystal size of $PbSO_4$ gives a smaller current because of the smaller reaction site area per unit volume.

Keywords: Lead acid battery reactions; Dissolution and precipitation reaction; Reaction site model

1. Introduction

The charge and discharge mechanisms of the positive and the negative electrodes in sulfuric acid solution are very important for the improvement of the lead acid battery. In this paper, research to clarify the reaction mechanisms of both electrodes is reviewed. The overall discharge reaction of the lead acid battery is given

$$\beta\text{-}PbO_2 + Pb + 2H_2SO_4 \rightarrow 2PbSO_4 + 2H_2 \quad (1)$$

$PbSO_4$ is formed on the positive and the negative electrodes resulting from the discharge of β-PbO_2 and Pb in sulfuric acid solution. These reactions proceed via dissolution–precipitation reactions, that is the formation of Pb^{2+} ions by an electron-transfer step followed by the precipitation of $PbSO_4$. On charge, the inverse reactions proceed via dissolution–precipitation reactions, that is the formation of Pb^{2+} ions by a dissolution of $PbSO_4$ followed by the precipitation of β-PbO_2 or Pb by an electron-transfer step.

During the discharges on both β-PbO_2 and Pb electrodes, the large supersaturation of Pb^{2+} ions on the electrode surface may be obtained during the initial period by an electron-transfer reaction. $PbSO_4$ nuclei are then formed, and the precipitation of $PbSO_4$ proceeds smoothly on the $PbSO_4$ nuclei in sulfuric acid solution supersaturated with Pb^{2+} ions. The particle sizes of $PbSO_4$ precipitated during discharge, may be changed by the change of the concentrations of Pb^{2+} ions, and this parameter exercises an important influence on the discharge and charge performances. The concentration of Pb^{2+} ions is controlled by the concentration of sulfuric acid solution and the current density of discharge.

During charge on both $PbSO_4$ electrodes, Pb^{2+} ions are supplied from $PbSO_4$ crystals. Since $PbSO_4$ is a nonconducting ionic crystal, the anodic oxidation to β-PbO_2 and

0378-7753/00/$ - see front matter
PII: S0378-7753(99)00378-X

the cathodic reduction to Pb proceed at the interface between $PbSO_4$ crystal and β-PbO_2 or Pb on the grid alloy, which is an electronic conductor, and such reaction site areas are changed during the course of the reaction. Thus, besides the exchange current densities of the electrode reactions, the crystal size and the solubility of $PbSO_4$ in sulfuric acid solution and the diffusion coefficient and the length of the diffusion path of Pb^{2+} ions places important roles in the charge process.

2. The discharge reaction of the positive electrode (Cathodic reduction of β-PbO_2 to $PbSO_4$)[1]

Reaction mechanism was investigated by using a rotating ring-disk electrode. Both the ring and the disk were made of Pb (purity:99.9%). The disk was oxidized anodically in 0.5 M H_2SO_4 at 2 mA cm^{-2} for 2 h. The formation of β-PbO_2 on the Pb surface after such treatment was confirmed by X-ray analysis. Fig. 1 shows a cyclic voltammogram on a β-PbO_2 disc in 0.5 M H_2SO_4 and the ring current on Pb, which is kept at -1.02 V vs. Hg/Hg_2SO_4, corresponding to the reaction of the disk. The peak in the cathodic disk current is due to the formation of $PbSO_4$ during the discharge of PbO_2 and a broad peak in the anode current is due to the formation of PbO_2 during charge. This shows that the discharge and charge reactions are irreversible and the reaction rate of discharge is larger than that of charge. A peak in the ring current corresponding to a cathodic peak on the disk was observed during discharge, but the increase of cathodic ring current was observed during charge.

Thus, the dissolution of Pb^{2+} ions during discharge is different from that during charge. Though the theoretical ring current corresponding to a cathodic peak current of the disc is -18.3 mA, the observed current is only -4.0 mA. Moreover, though the solubility of $PbSO_4$ in 0.5 M H_2SO_4 is 1.88×10^{-5} M, the concentration of Pb^{2+} ions on the disk is 2.65×10^{-2} M. This shows that not all of the Pb^{2+} ions generated during discharge diffuse out into the sulfuric acid solution, but they do dissolve more than the equilibrium concentration. Such a large supersaturation of Pb^{2+} ions can be understood only in terms of the dissolution–precipitation mechanism.

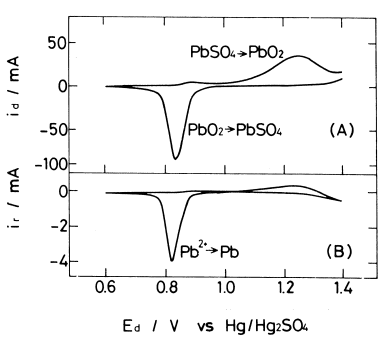

Fig. 1. (A) Cyclic voltammogram on PbO_2 disk in 0.5 M H_2SO_4 scanned between 0.6 V and 1.4 V vs. Hg/Hg_2SO_4 at scan rate of 10 mV s^{-1} and a rotation speed of 2000 rev min^{-1}. (B) Ring current corresponding to the reaction of the disk.

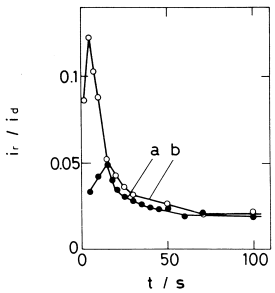

Fig. 2. Change of i_r / i_d during potentiostatic discharges calculated from the disk currents at 1500 rev min^{-1} and ring currents corresponding to the reaction of the disk in 0.5 M H_2SO_4. a: 0.85 V; b: 0.80 V vs. Hg/Hg_2SO_4.

From the changes in the disk current (i_d) and the ring current (i_r) at potentiostatic discharge, the value of i_r/i_d corresponds to the ratio of the formation rate of Pb^{2+} ions to the precipitation rate and is shown in Fig. 2. The precipitation rate during the initial period is smaller than the formation rate due to the absence of $PbSO_4$ nuclei on the electrode surface. The values of i_r/i_d increase after the formation of $PbSO_4$ nuclei, and then decrease until the value reaches 0.03 due to the increase of the precipitation rate. This value, which is smaller than the theoretical value of 0.145, shows that the precipitation rate is much larger than the formation rate.

Fig. 3 shows the concentration of Pb^{2+} ions on the electrode surface in different concentrations of sulfuric acid, calculated from the ring current in the steady state during galvanostatic discharge at 1 mA/0.4 cm^2. The concentration of Pb^{2+} ions at each concentration of sulfuric acid is higher than the solubility of $PbSO_4$, as shown in Table 1 from Refs. [2,3]. This may be due to the formation of a colloidal compound with Pb^{2+} ions. The concentration of Pb^{2+} ions in 1.0 M H_2SO_4 was the largest found

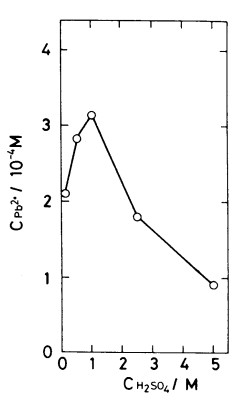

Fig. 3. Concentration of Pb^{2+} ions on the electrode surface during discharge at 1.0 mA/0.4 cm^2 in different concentrations of sulfuric acid.

Table 1
The concentrations of Pb^{2+} and H^+ ions in various sulfuric acid concentrations

$C_{H_2SO_4}$/M	$C_{Pb^{2+}}/10^{-5}$ M	C_{H^+}/M
0.1	1.58	0.0293
0.5	1.88	0.0793
1.0	2.40	0.1335
2.5	1.60	0.3667
5.0	0.56	1.6540

among five different acid concentrations, and this may be related to the stability of the formation of a colloidal compound.

Fig. 4 shows scanning electron micrographs of $PbSO_4$ crystals formed during galvanostatic discharge in various electrolytes. The largest crystal size was obtained in 0.5 M H_2SO_4 with the largest Pb^{2+} ion concentration on the surface. Since the colloidal compound in 0.5 M H_2SO_4 may be unstable, the number of $PbSO_4$ nuclei generated on the electrode surface may be less than those in other electrolytes. In this way, the concentration of Pb^{2+} ions on the surface during discharge is the important factor to determine the particle size of $PbSO_4$ crystals formed on the electrode surface.

Fig. 5 shows scanning electron micrographs of $PbSO_4$ crystals by galvanostatic discharge in 5.0 M H_2SO_4 at 0.5, 1.0, 5.0 and 10.0 mA cm^{-2}. A large discharge current resulted in a large supersaturation of Pb^{2+} ions on the electrode surface and caused the formation of a lot of $PbSO_4$ nuclei. On the other hand, the large supersaturation of Pb^{2+} ions could not be generated by a small current discharge. Thus, the crystal size of $PbSO_4$ increases with a decreasing discharge current.

If the discharge capacity is limited by the passivation of the electrode surface with $PbSO_4$ crystals, the condition forming the large $PbSO_4$ crystals may be favoured.

3. The discharge reaction of the negative electrode (anodic oxidation of Pb to $PbSO_4$)[4]

Pb rod (purity: 99.9%, diameter: 6 mm) was used. It was mounted in a polytetrafluoroethylene tube and was polished with emery paper and then etched in a dilute nitric acid solution. After these treatments it was immersed in sulfuric acid solution, and was then held at −1.3 V vs. Hg/Hg_2SO_4 for a few minutes to removed the residual lead sulfate crystals before experiment.

Pb is discharged in sulfuric acid solution through the formation of Pb^{2+} ion by an electron-transfer step followed by the precipitation of $PbSO_4$. Apart from the fact that the exchange current density of the anodic oxidation of Pb may be larger than that of the cathodic reduction of β-PbO_2, Pb is discharged by the same process as the discharge of β-PbO_2.

Fig. 6 shows scanning electron micrographs of $PbSO_4$ crystals formed during galvanostatic discharge in various conditions. The size of $PbSO_4$ crystals in 0.5 M H_2SO_4 was larger than that in 5 M H_2SO_4, in the case of galvanostatic discharge at 1.0 mA cm^{-2}. Crystals prepared by the discharge at 0.1 mA cm^{-2} were marginally larger than those prepared by the discharge at 1.0 mA cm^{-2}, in the case of discharge in 0.5 M H_2SO_4. Since the concentration of Pb^{2+} ions on the electrode surface during steady state discharge in 0.5 M H_2SO_4 was larger than that in 5 M H_2SO_4, the largest crystal size was obtained in 0.5 M H_2SO_4. The $PbSO_4$ formed during the discharge depend on the formation of the nuclei and the crystal growth. A lot of nuclei are formed on the electrode surface at a high current discharge. So, the size of $PbSO_4$ crystals tends to become smaller at a high current discharge.

4. The charge reaction of the positive electrode (anodic oxidation of $PbSO_4$ to β-PbO_2)[5–7]

The surface of a Pb rod as used in Section 3 was oxidized to PbO_2 in 0.5 M H_2SO_4 at 1 mA cm^{-2} for about 24 h, and then galvanostatically discharged at 1 mA cm^{-2} in 0.5 M H_2SO_4. The discharge–charge cycle was continued until the capacity of the PbO_2 electrode increased to 40 mA min.

Fig. 7 shows the potentiodynamic current–voltage curves which were obtained after the subtraction of the oxygen evolution current from the whole anodic current.

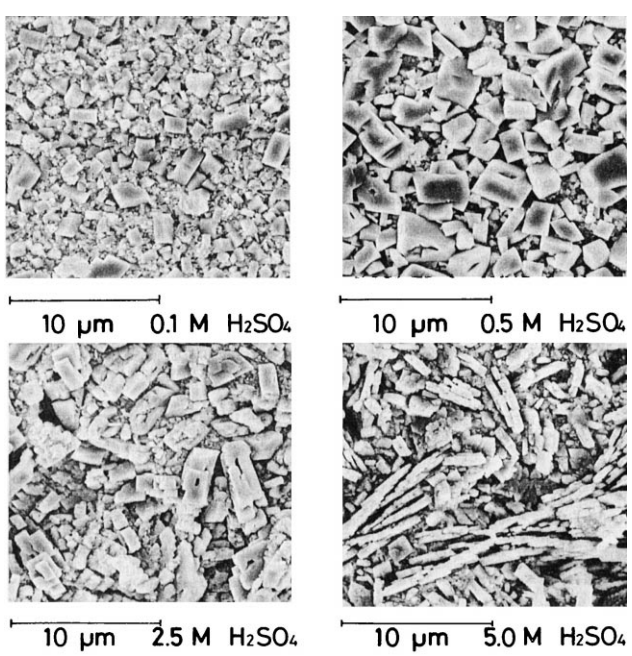

Fig. 4. Scanning electron micrographs of the electrode surface after discharge of PbO_2 at 1.0 mA/0.4 cm^2 in different concentrations of sulfuric acid.

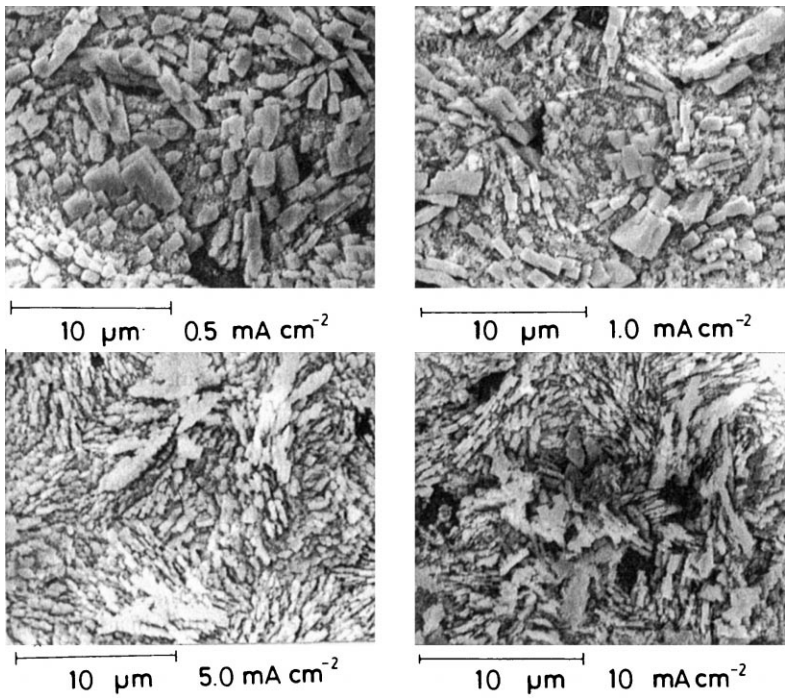

Fig. 5. Scanning electron micrographs of the electrode surface after discharge of PbO_2 in 5.0 M H_2SO_4 at different current densities.

Symmetric current–potential curves were observed. Such curves are similar to those for a surface reaction rather than a diffusion-controlled electrode reaction. The peak potential shifted to a more anodic potential upon increasing the sweep rate, and the half-wave width became larger with increasing sweep rate. These results indicate that the charge-transfer process of the oxidation of $PbSO_4$ to β-PbO_2 is very slow.

However, it is difficult to treat the oxidation of $PbSO_4$ to β-PbO_2 quantitatively, because a large ionic crystal with neither electronic nor ionic conductivity would not be able to oxidize in the same way as would a soluble species. The dissolving Pb^{2+} ions from $PbSO_4$ crystal are oxidized to Pb^{4+} ions and react with H_2O to precipitate on the electrode surface as β-PbO_2. Conditions for the oxidation of $PbSO_4$ are not equal over the electrode surface, and the high oxidation rate is sustained by the high concentration of Pb^{2+} ions on the β-PbO_2. Thus, the reaction site is considered to be the interface between β-PbO_2 and $PbSO_4$. At such an interface, Pb^{2+} ions can be adequately supplied from the $PbSO_4$ crystal, and a charge transfer reaction can occur on β-PbO_2.

Fig. 8 shows potentiodynamic current–voltage curves for the oxidation of $PbSO_4$ formed by galvanostatic discharge at 0.5, 1.0 and 10.0 mA cm^{-2} in 5.0 M H_2SO_4. The anodic peak potential shifted to a more positive value upon decreasing the discharge current. This shows the oxidation of $PbSO_4$ formed under a low discharge current

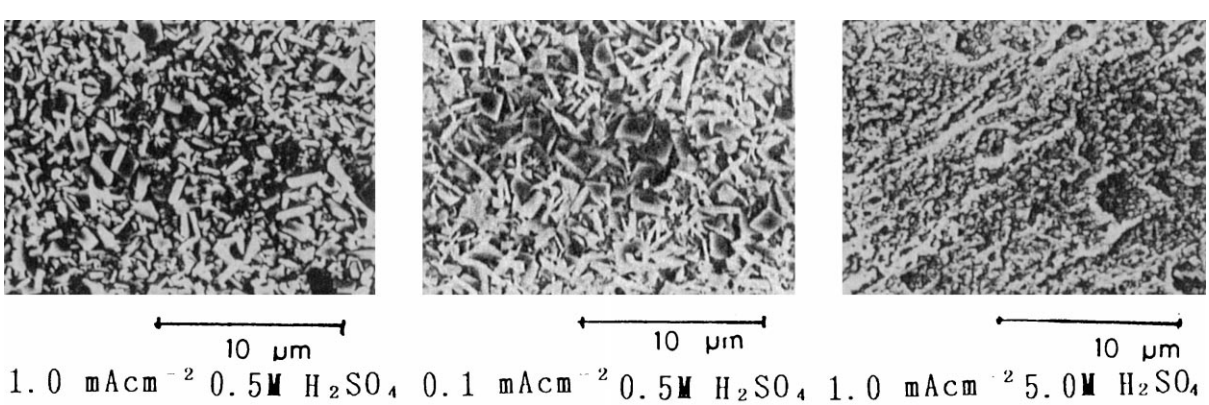

Fig. 6. Scanning electron micrographs of the electrode surface after galvanostatic discharge of Pb in sulfuric acid solution under different conditions.

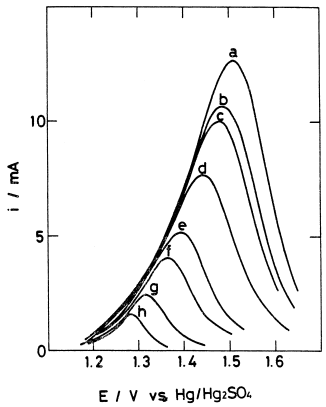

Fig. 7. Potentiodynamic current–voltage curves in 5.0 M H_2SO_4 of β-PbO_2 electrode discharged at 10 mA cm^{-2} in 5.0 M H_2SO_4 at various sweep rates. sweep rate: a: 10; b: 8; c: 7; d: 5; e: 3; f: 2; g: 1; h: 0.5 mV s^{-1}.

is more difficult than that formed at a high discharge current. The size of the $PbSO_4$ formed at a low discharge current was very large, as already shown in Fig. 5. Thus, increasing the $PbSO_4$ crystal size caused difficulty with regard to the oxidation of $PbSO_4$. Fig. 9 shows potentiodynamic current–voltage curves for the oxidation of $PbSO_4$ formed by galvanostatic discharge at 1.0 mA cm^{-2} in 5.0 M and 0.5 M H_2SO_4 for 60 s. Both electrodes were oxidized in 5.0 M H_2SO_4 by a potential sweep method. The oxidation rate of $PbSO_4$ formed in 5.0 M H_2SO_4 was larger than that in 0.5 M H_2SO_4. The size of the $PbSO_4$ depends on the concentration of the sulfuric acid solution, as already shown in Fig. 4. In this case, the size of the $PbSO_4$ formed in 5.0 M H_2SO_4 was less than that in 0.5 M H_2SO_4. Thus, the reaction rate of the oxidation of the $PbSO_4$ depends on the crystal size of the $PbSO_4$ precipitated on the electrode surface during discharge. This indicates that the reaction site at which a high reaction rate is sustained is the interface between $PbSO_4$ and β-PbO_2.

Such reaction site was examined by using the β-PbO_2 electrode prepared by electrodeposition onto a gold plate from 2.5 M HNO_3 containing 0.03 M $Pb(NO_3)_2$ for 30 min at 3 mA cm^{-2}. The thickness of the lead dioxide on

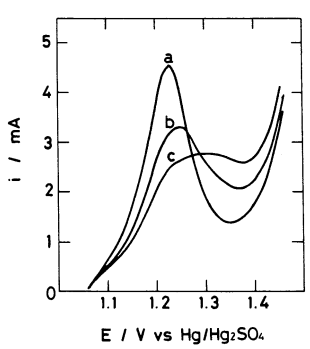

Fig. 8. Potentiodynamic current–voltage curves at sweep rate of 1 mV s^{-1} for the oxidation of $PbSO_4$ formed by galvanostatic discharge at various current densities in 5.0 M H_2SO_4. discharge current: a: 10.0; b: 1.0; c: 0.5 mA cm^{-2}.

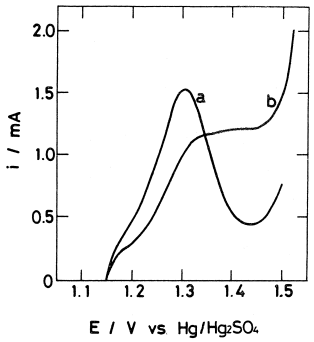

Fig. 9. Potentiodynamic current–voltage curves in 5.0 M H_2SO_4 at sweep rate of 1 mV s^{-1} for the oxidation of $PbSO_4$ formed galvanostatic discharge at 1.0 mA cm^{-2} for 60 s in various concentrations of H_2SO_4. concentration of H_2SO_4: a: 5.0 M; b: 0.5 M H_2SO_4.

the gold plate was about 7 μm. The electrode was discharged at 0.1 mA cm^{-2} in 0.5 M H_2SO_4 until 0.8 V vs. Hg/Hg_2SO_4, after immersion in 0.5 M H_2SO_4 for about 30 min.

Fig. 10 shows the current time transient in 0.1 M, 0.5 M, 1.0 M, 2.5 M, and 5.0 M H_2SO_4 during the potentiostatic oxidation at (Ee + 0.2)V vs. Hg/Hg_2SO_4, where Ee is an equilibrium potential of the β-PbO_2 electrode in each concentration of sulfuric acid solution. All the transients consisted of both rising and falling parts. The anodic current in 0.5 M H_2SO_4 was the largest of five transients. The oxidation of lead sulfate film to β-PbO_2 depends on the concentration of the sulfuric acid solution, and its rate is fastest in 0.5 M H_2SO_4. The oxidation of lead sulfate proceeded through the dissolution–precipitation mechanism at the interior of the film, written as follows,

$$PbSO_4 \rightarrow Pb^{2+} + SO_4^{2-} \quad (2)$$

$$Pb^{2+} + 2H_2O \rightarrow \beta\text{-}PbO_2 + 4H^+ + 2e^- \quad (3)$$

and then the following equation for the anodic current may be written,

$$i = nFA(t)\, kC_{Pb^{2+}}^{x} C_{H^+}^{-y} \quad (4)$$

where $A(t)$ is the reaction interface area, which changes with the proceeding oxidation, $C_{Pb^{2+}}$ and C_{H^+} are the

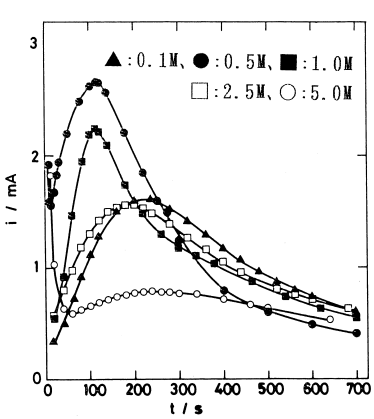

Fig. 10. The current–time transients for the oxidation of $PbSO_4$ to β-PbO_2 at (Ee + 0.2)V in various sulfuric acid concentrations.

concentration of Pb^{2+} ion and H^+ ion in the sulfuric acid solution. These concentrations depend on the concentration of sulfuric acid solution, x and $-y$ are the reaction order of Pb^{2+} ion and H^+ ion respectively for the anodic reaction. k is the potential dependence constant. The anodic current, i, depends on the concentrations of sulfuric acid solution and the reaction area. The Pb^{2+} and H^+ ion concentrations in various sulfuric acid concentrations are already shown in Table 1. The rate of the charge reaction may be mainly determined by the concentration of the Pb^{2+} ion. But the peak current in 0.5 M H_2SO_4 was larger than that in 1.0 M H_2SO_4. Thus, the H^+ ion concentration reflects the peak current.

The change of the reaction interface area during the oxidation of $PbSO_4$ is also obvious from the scanning electron micrographs of the surface, the cross section, and the interface between a gold substrate and the lead sulfate film of the electrode oxidized at 1.11 V [(Ee + 0.2)V] vs. Hg/Hg_2SO_4 to 20, 50 and 100% of the electricity passed during the discharge, as shown in Fig. 11. The electrode surface oxidized to 20% was perfectly covered with very large lead sulfate crystals, whose size was about

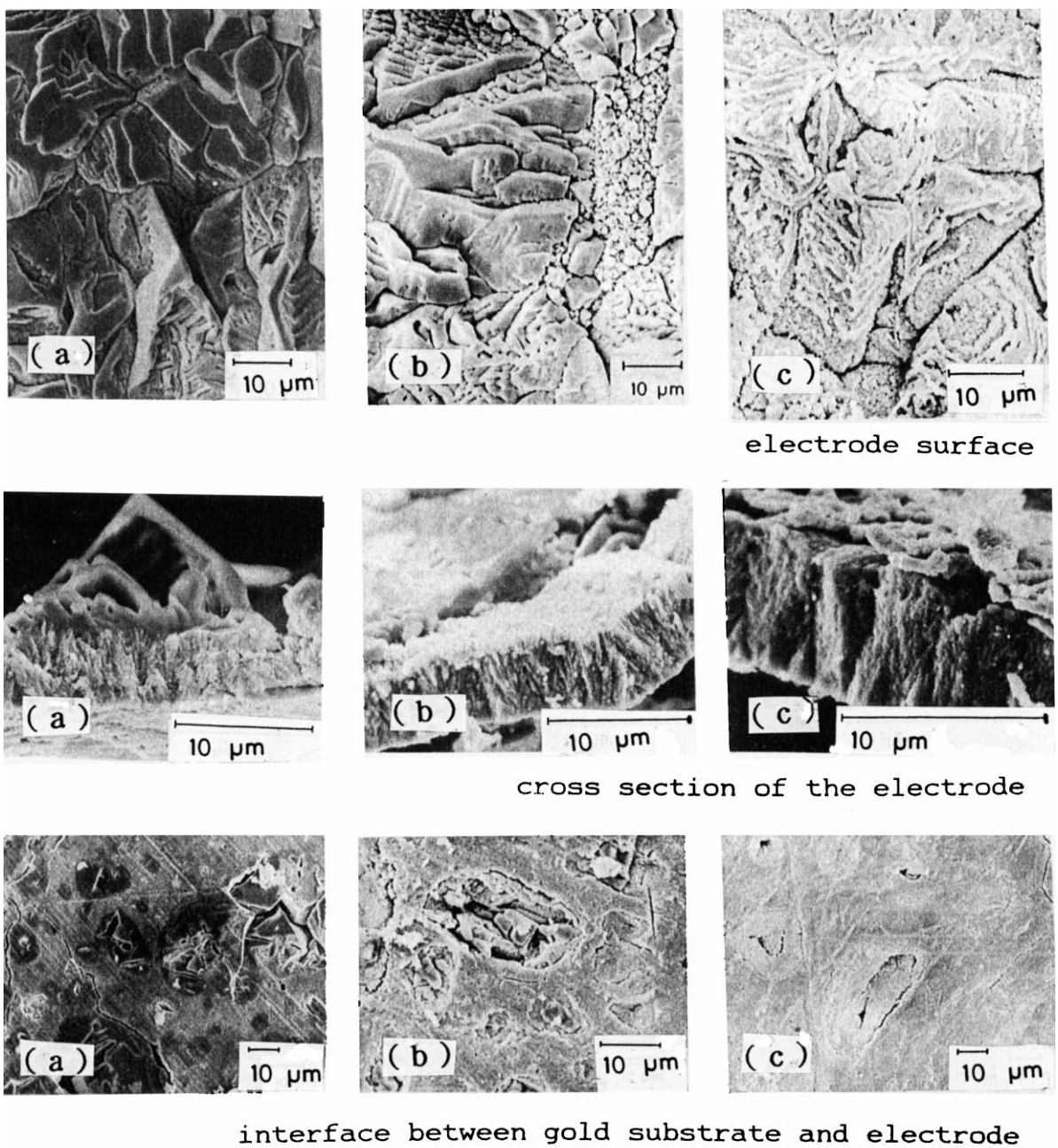

Fig. 11. Scanning electron micrographs of the electrode surface, the cross section of the electrode, and the interface between a gold substrate and the lead sulfate film oxidized at 1.11 V to (a) 20%, (b) 50%, and (c) 100% of the discharge capacity.

20–30 μm. At 50% the lead dioxide crystals appeared on the electrode surface, but the ratio of the surface areas of lead dioxide and lead sulfate was smaller than 50%. At 100% all parts of the electrode surface covered with lead dioxide. The lead dioxide layer was observed in the cross section of the electrode oxidized to 20% and lead sulfate was present on the lead dioxide layer. At 50% lead sulfate near the electrode surface was oxidized to lead dioxide. The lead sulfate was observed at 20%, but it was not observed beyond 50%, on the interface between a gold plate and the lead sulfate film. From these micrographs, the oxidation of a lead oxidation takes place in the deepest parts of the lead sulfate film to lead dioxide, consisted of three steps, as illustrated schematically in Fig. 12: (i) The film, and the lead dioxide layer at the interface between a gold plate and the lead sulfate is formed; (ii) The oxidation proceeds at the interior of the film where the two-dimensional change of the reaction interface area and the thick lead dioxide layer grows; and (iii) Lead sulfate remaining near the interface between the electrolyte and the electrode is oxidized without an increase of the reaction interface area. The rising and falling current–time transient of Fig. 10 seems to corresponds to the growth of the lead dioxide layer at the interior of the lead sulfate film.

5. The charge reaction of the negative electrode (Cathodic reduction of $PbSO_4$ to Pb)[4]

The Pb rod as used in Section 3 was used. Fig. 13 shows potentiodynamic current–voltage curves during the cathodic scan of the $Pb/PbSO_4$ electrode in 1.0 M H_2SO_4 at various sweep rates. The cathodic current rapidly increased at about -0.98 V vs. Hg/Hg_2SO_4 and then gradually decreased. In the case of the oxidation of $PbSO_4$ as explained in Section 4, such a rapid increase in current was not observed.

Thus, the reaction site model illustrated in Fig. 14 was proposed. In this model, it is assumed that the Pb^{2+} ions are transported from the $PbSO_4$ crystal surface to the Pb

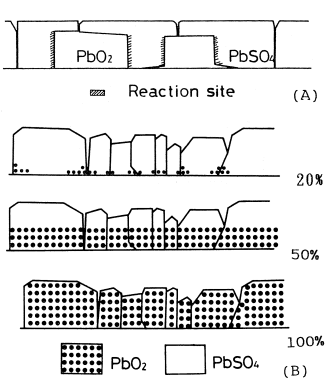

Fig. 12. (A) Schematic representation of the reaction site for the charging reaction of the β-PbO_2 /$PbSO_4$ electrode (B) Schematic illustration of the model for the oxidation of $PbSO_4$ film to β-PbO_2 in three step.

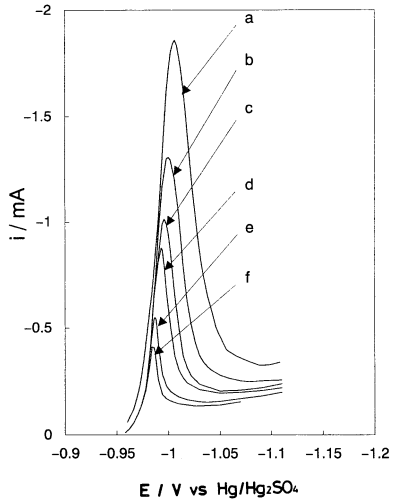

Fig. 13. Potentiodynamic current–voltage curves in 1.0 M H_2SO_4 of the cathodic reduction of $PbSO_4$ to Pb electrode prepared by galvanostatic discharge at 1.0 mA cm^{-2} for 2 min in 1.0 M H_2SO_4 at various sweep rates. sweep rate: a: 20; b: 10; c: 7; d: 5; e: 2; f: 1 mV s^{-1}

surface and then are reduced. The reaction rate depends on the electrochemical kinetic parameters, e.g., the exchange charge transfer rate, the real area of the interface between Pb and $PbSO_4$, and the mass-transfer of Pb^{2+} ions. The gap between the Pb and $PbSO_4$, as shown in Fig. 14(c), may be narrow, and the diffusion phenomena in such a gap can be assumed to be like those in a thin layer cell. The concentration profile of Pb^{2+} ions is illustrated in Fig. 14(d), and the $PbSO_4$ crystal becomes smaller as shown in Fig. 14(b).

In this model, the diffusion current, i, is obtained from

$$i = 2FDA(t)\left[C_{Pb^{2+}*} - C_{Pb^{2+}}\right]/l \quad (5)$$

where l is the gap distance between the lead and the lead sulfate and $A(t)$ is the area of the interface region, $C_{Pb^{2+}}$

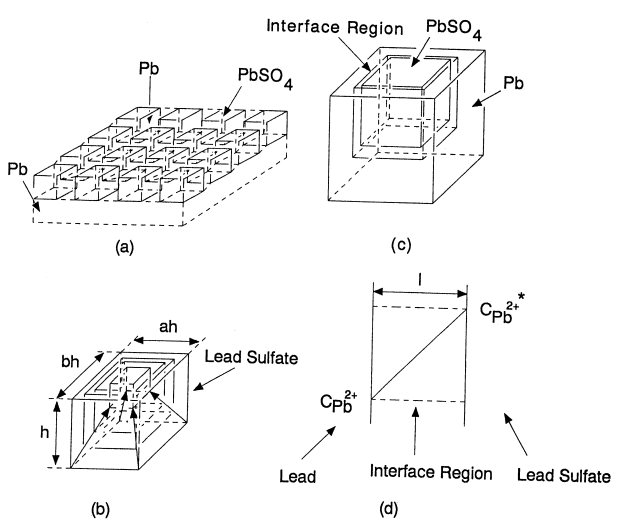

Fig. 14. (a) Schematic illustration of the lead sulfate crystals deposited on the lead surface. (b) The change of the lead sulfate crystal during the cathodic reduction. (c) The model of the reaction site. (d) Concentration profile of lead ion at the interface region.

is the concentration of Pb^{2+} ions at the lead surface and $C_{Pb^{2+}*}$ is the concentration of Pb^{2+} ions at equilibrium (solubility of $PbSO_4$). The effective gap distance was assumed to be constant, and $A(t)$ was calculated using the following empirical equation

$$A(t) = [2(a+b) + ab]\,x^2 \quad (6)$$

where the lead sulfate crystal is assumed to be an oblong box, *ax* long by *bx* wide by *x* deep. With such assumptions, the current–voltage curve for a single lead sulfate crystal was calculated. The total current was calculated by the multiplication of the number of lead sulfate crystals.

Since the exchange current density is estimated to be the order of 1–10 mA cm^{-2} [8,9], the rate-determining step for the reduction of $PbSO_4$ to Pb is controlled by mass-transfer. Then, current–voltage curves were calculated at various sweet rates, under the following conditions: concentration of Pb^{2+} ions: 2.4×10^{-5} M, the diffusion coefficient: 5×10^{-6} cm^2 s^{-1}, height: 1 μm, length: 1 μm, width: 1 μm, diffusion path length: 5×10^{-3} μm, and the volume of $PbSO_4$ crystal: 1.2×10^{-6} cm^3, and these curves are shown in Fig. 15. The calculated curves are similar to those measured in Fig. 13. However, the observed curves showed some deviation from the calculated curves. These deviations may be due the distribution of $PbSO_4$ crystal sizes and the uncertainty of estimating the number of these crystals.

From the above model, it can be expected that the large crystal size gives a smaller current because of the smaller reaction site area per unit volume, and a large solubility of $PbSO_4$ gives a large current. Thus, the peak current in the current–potential curves of the cathodic reduction of $PbSO_4$ crystals depends on the crystal size and the solubility of $PbSO_4$ crystal in sulfuric acid. Fig. 16 shows current–voltage curves for the $Pb/PbSO_4$ electrode in 0.5 M H_2SO_4 at 10 mV s^{-1}, which were prepared by the galvanostatic discharge of Pb at 1.0 mA cm^{-2} for 20 s in 0.5 M and 5.0 M H_2SO_4. From Fig. 16, it can be seen that the current in 5.0 M H_2SO_4 is much larger than that in 0.5 M H_2SO_4. The solubility in 5.0 M H_2SO_4 is one-third of that in 0.5 M H_2SO_4, and the crystal size in 5.0 M H_2SO_4 is smaller than that in 0.5 M H_2SO_4, as already shown in Fig. 6. From the comparison of experimental results with the expected peak current it can be seen that the size of the crystals has a greater effect on the reaction current than the solubility of the crystals. Since a lot of nuclei are formed

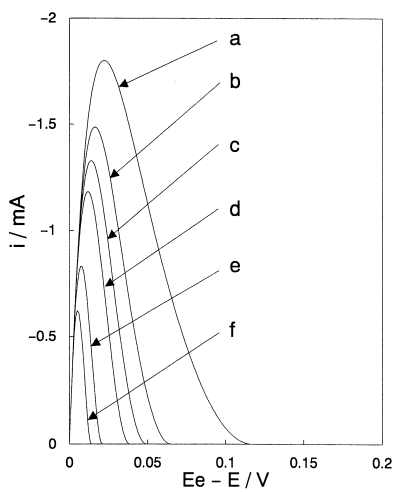

Fig. 15. Calculated current–voltage curves for the cathodic reduction of $PbSO_4$ to Pb at various sweep rates. sweep rate: a: 20; b: 10; c: 7; d: 5; e: 2; f: 1 mV s^{-1}.

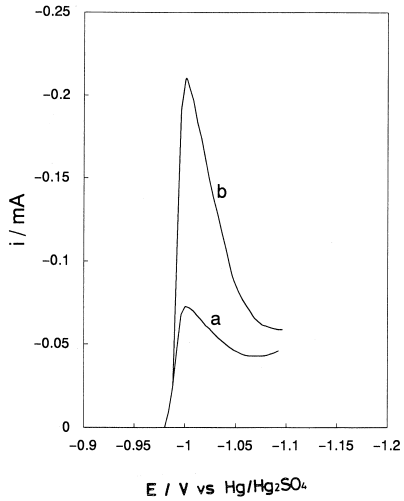

Fig. 16. Current–voltage curves for the cathodic reduction of $PbSO_4$ crystals in 0.5 M H_2SO_4 at 10 mV s^{-1}, $Pb/PbSO_4$ electrodes were prepared by the galvanostatic discharge at 1.0 mA cm^{-2} for 20 s in (a) 0.5 M and (b) 5.0 M H_2SO_4.

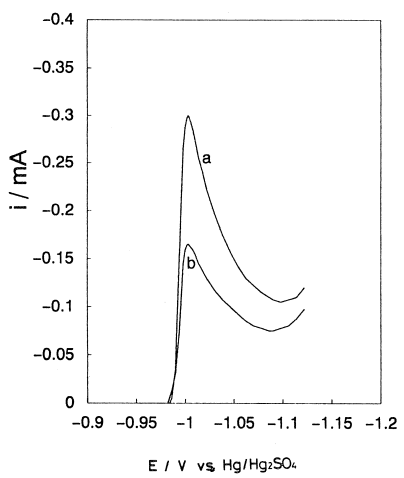

Fig. 17. Current–voltage curves for the cathodic reduction of $PbSO_4$ crystals at 10 mV s^{-1}, $Pb/PbSO_4$ electrodes were prepared by the galvanostatic discharge in 0.5 M H_2SO_4 at (a) 1.0 mA cm^{-2} for 30 s, and (b) 0.1 mA cm^{-2} for 300 s.

on the electrode surface at a high discharge current, the $PbSO_4$ crystal becomes smaller at a high current discharge, as already shown in Fig. 6. Fig. 17 shows current–voltage curves for the $Pb/PbSO_4$ electrode in 0.5 M H_2SO_4 at 10 mV s^{-1}, which were prepared by galvanostatic discharge at 1.0 mA cm^{-2} for 30 s and 0.1 mA cm^{-2} for 300 s in 0.5 M H_2SO_4. The biggest observed difference is the crystal size of $PbSO_4$. Thus it can be seen that the electrochemical reaction of $Pb/PbSO_4$ strongly depends on crystal size. Then, the peak currents increased with increasing diffusion coefficient and increased with decreasing diffusion path length. The diffusion coefficient of Pb^{2+} ions does not depend much upon concentration and it will not influence the reduction of $PbSO_4$. If a $PbSO_4$ crystal is isolated in a porous lead electrode, the $PbSO_4$ crystal may not be completely reduce during a potential sweep from Ee to Ee + 0.2 V at 10 mV s^{-1}.

References

[1] Z. Takehara, K. Kanamura, Electrochim. Acta 29 (1984) 1643–1648.
[2] G.W. Vinal, D.N. Craig, J. Res. Natl. Bur. Stand. 22 (1939) 55.
[3] B. Bode, Lead-Acid Batteries, Wiley, New York (1977).
[4] K. Kanamura, Z. Takehara, J. Electrochem. Soc. 139 (1992) 345–351.
[5] Z. Takehara, K. Kanamura, Bull. Chem. Soc. Jpn. 60 (1987) 1567–1572.
[6] Z. Takehara, K. Kanamura, J. Electrochem. Soc. 134 (1987) 13–18.
[7] Z. Takehara, K. Kanamura, J. Electrochem. Soc. 134 (1987) 1604–1610.
[8] S. Haruyama, J. Electrochem. Soc. Jpn. 35 (1967) 62.
[9] N.A. Hampson, D. Larkin, Trans. Faraday Soc. 65 (1969) 1.